

## EXPERIMENTAL SECTION

### Materials

Commercially available WO<sub>2.72</sub> Powder was purchased from Xiangtian Nano MaterialS Co., Ltd. (Shanghai). Ethanol used in all experiments was purchased from Sinopharm Chemical Reagent Co., Ltd. (China). CO<sub>2</sub> with purity of 99.99% was provided by the Zhengzhou Shuangyang Gas Co. and was used as received.

### Fabrication of amorphous WO<sub>2.72</sub>

In brief, 1.0 g of commercial WO<sub>2.72</sub> powder was initially dispersed into 200 mL of ethanol/water mixtures with ethanol volume fractions of 50%. Then the dispersion was transferred into the supercritical CO<sub>2</sub> (SC CO<sub>2</sub>) apparatus composed mainly of a stainless-steel autoclave (50 mL) with a heating jacket and a temperature controller. The autoclave was heated to 40 °C and CO<sub>2</sub> was injected into the autoclave until to a required pressure (16 MPa). After a reaction time of 6 h, the gas was released. Subsequently, the dispersion was collected was centrifuged at 5000 rpm for 10 min to remove aggregates, and the supernatant was collected to centrifuge again at 10000rpm for 10min. Finally, the supernatant was collected to dry at 60°C. Different contrast experiments were carried out under the different experiment conditions, such as the varied SC CO<sub>2</sub> pressure and temperature.

## **Characterization**

Transmission electron microscopy (TEM) and high-resolution TEM (HRTEM) characterizations were performed with a JEM-2100. XRD patterns were recorded using a Y-2000 X-ray Diffractometer with Cu K $\alpha$  radiation. X-ray photoemission spectroscopy (XPS) was performed using ESCLAB 280. The absorbance data were measured with an UV-vis-NIR spectrophotometer (UV-vis DRS, Cary 500). Raman spectra measurements were performed on Lab RAM HR Evolution using laser wavelength of 532 nm. The IR camera (FLIR-E6390) was used to test the temperatures under the light irradiation.

## **Photothermal experiments**

The photothermal effect was measured by monitoring the temperature of the samples in deionized (DI) water at various concentrations (0, 0.1, 0.3, 0.5, 0.7, and 1.0 mg/mL). Briefly, 1.0 mL of the sample dispersion in a glass cuvette (total volume of 2 mL) was irradiated by the 808 nm laser ( $1.06 \text{ W} \cdot \text{cm}^{-2}$ ), and the temperature of the solution was measured every 30s by a thermocouple microprobe submerged in the solution. The temperature of 1.0 mL of DI water upon the same irradiation was measured as a control experiment. To evaluate the single wavelength photothermal conversion efficiency, the dispersion was irradiated under the 808 nm laser ( $1.06 \text{ W} \cdot \text{cm}^{-2}$ ) for 720s. After switching off the laser, the temperature was further

measured. Single wavelength photothermal conversion efficiency ( $\eta$ ) was then calculated according to the reported method. To investigate the photothermal stability of the sample, the sample dispersion (1.0mg/mL, 1.0 mL) was irradiated by the 808 nm laser ( $1.06 \text{ W}\cdot\text{cm}^{-2}$ ) for 720s, and then the laser was off. Such cycle was repeated for 6 times.

### **Calculation of the photothermal conversion efficiency**

To quantitatively evaluate the photothermal conversion capability, we then measured the photothermal conversion efficiency ( $\eta$ ) of the sample. According to the literature,  $\eta$  can be calculated according to the following equation:

(1)

$$\eta = \frac{hA(\Delta T_{max} - \Delta T_{max, H_2O})}{I(1 - 10^{-A_\lambda})}$$

Where  $h$  is the heat transfer coefficient,  $A$  is the surface area of the container,  $\Delta T_{max}$  and  $\Delta T_{max, H_2O}$  are the temperature change of the sample dispersion and deionized water at the maximum steady state temperature, respectively,  $I$  is the 808 nm NIR laser power, and  $A_\lambda$  is the absorbance of the sample dispersion at 808 nm wavelength. In this equation, only  $hA$  is unknown. So  $\theta$  is introduced, which is defined as the ratio of  $\Delta T$  to  $\Delta T_{max}$ .

(2)

$$\theta = \frac{\Delta T}{\Delta T_{max}}$$

The total energy balance of this system as following equation:

(3)

$$\sum_i m_i C_{p,i} \frac{dT}{dt} = Q_A + Q_H - Q_{loss}$$

Where  $m$  and  $C_p$  are the mass and heat capacity, respectively. The suffix “i” of  $m$  and  $C_p$  refers to solvent (water) and dispersed matter.  $T$  is the solution temperature.  $Q_A$  is the photothermal energy absorbed by sample per second.  $Q_H$  is the heat associated with the light absorbed by water solvent per second.  $Q_{loss}$  is the thermal energy lost to the surroundings.

When the laser was shut off, the  $Q_A + Q_H = 0$ . Substituting equation (2) into equation (3),

(4)

$$t = - \frac{\sum_i m_i C_{p,i}}{hA} \ln \theta$$

Where  $\frac{\sum_i m_i C_{p,i}}{hA}$  can be calculated by linear relationship of time versus  $\ln \theta$ . Mass of sample ( $1 \times 10^{-6}$  Kg) is far less than that of water solvent ( $1 \times 10^{-$

<sup>3</sup> Kg), and the specific heat of water is much higher than other materials.

Therefore, the  $m_A$  and  $C_{p,A}$  of sample are neglected.  $m_{H_2O}$  is  $1 \times 10^{-3}$  Kg,

$C_{p,H_2O}$  is  $4.2 \times 10^3$  J/Kg °C. So hA value can be got in this way, and the

photothermal conversion efficiency ( $\eta$ ) could be calculated.

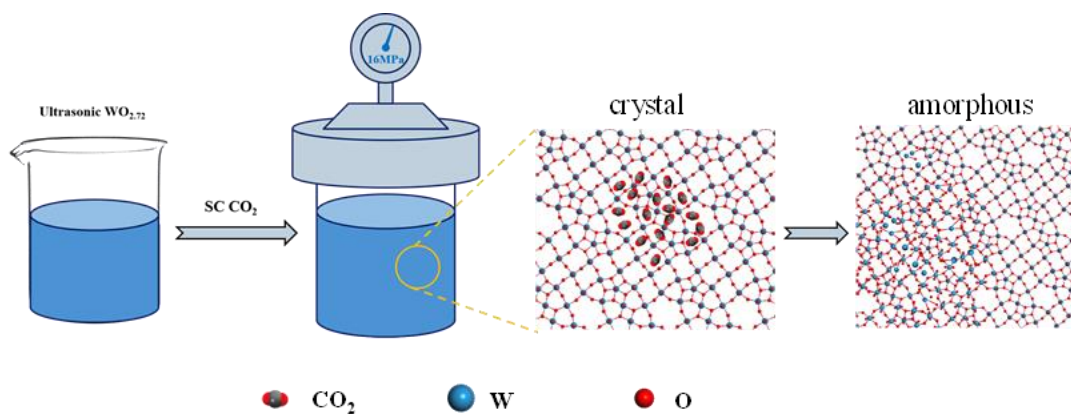


Figure. S1 schematically illustrates the fabrication procedure and amorphization of pristine  $\text{WO}_{2.72}$  sample with assistance of SC  $\text{CO}_2$ .

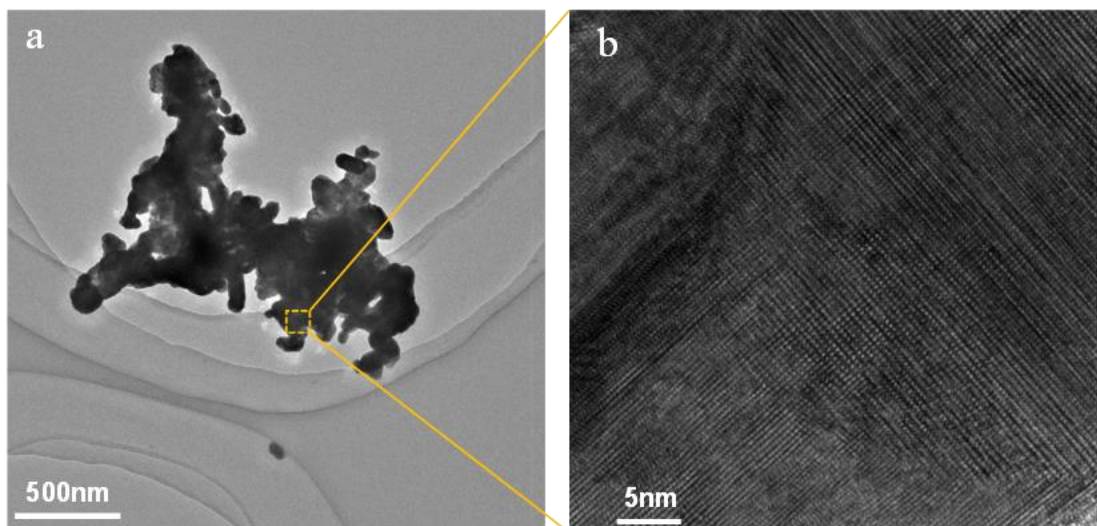


Figure S2. (a) TEM images of pristine  $\text{WO}_{2.72}$  sample. (b) HRTEM image of the region enclosed by the yellow square in (a).

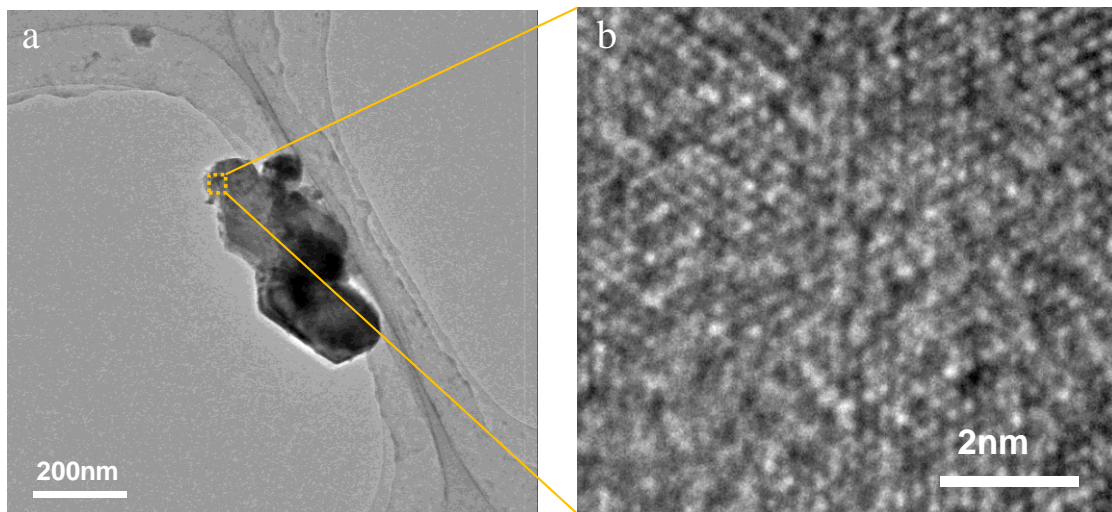


Figure S3. (a) TEM images of SC CO<sub>2</sub> treated sample. (b) HRTEM image of the region enclosed by the yellow square in (a).

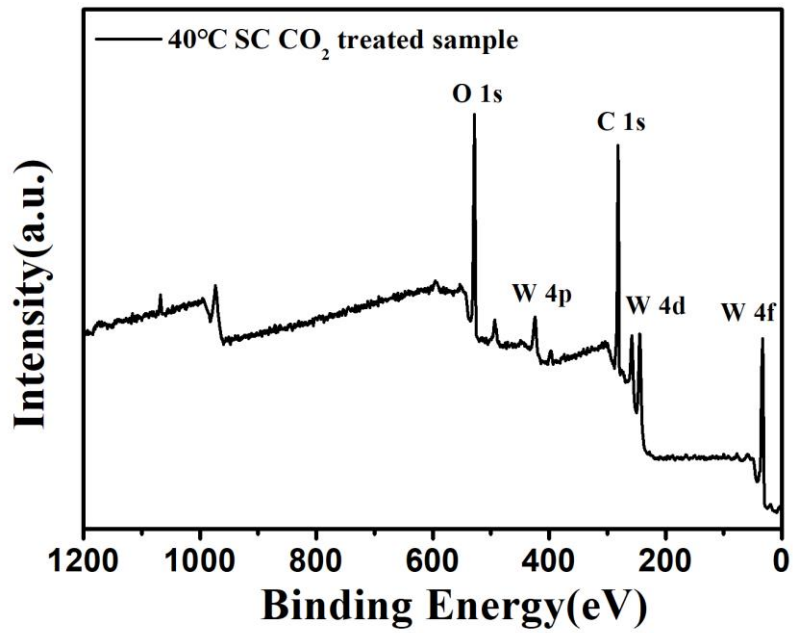


Figure S4. XPS survey spectrum for SC CO<sub>2</sub> treated sample.

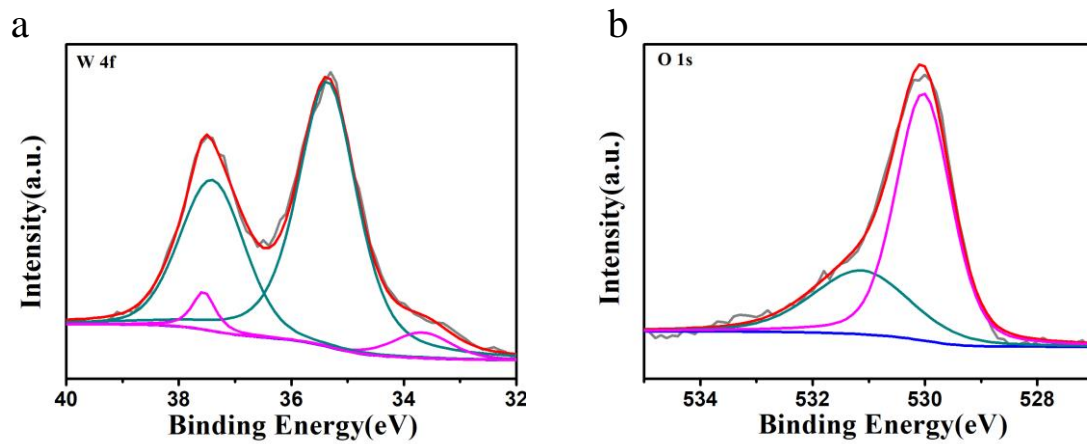


Figure S5. XPS spectra of pristine  $\text{WO}_{2.72}$  sample in the (a) W 4f and (b) O 1s regions.

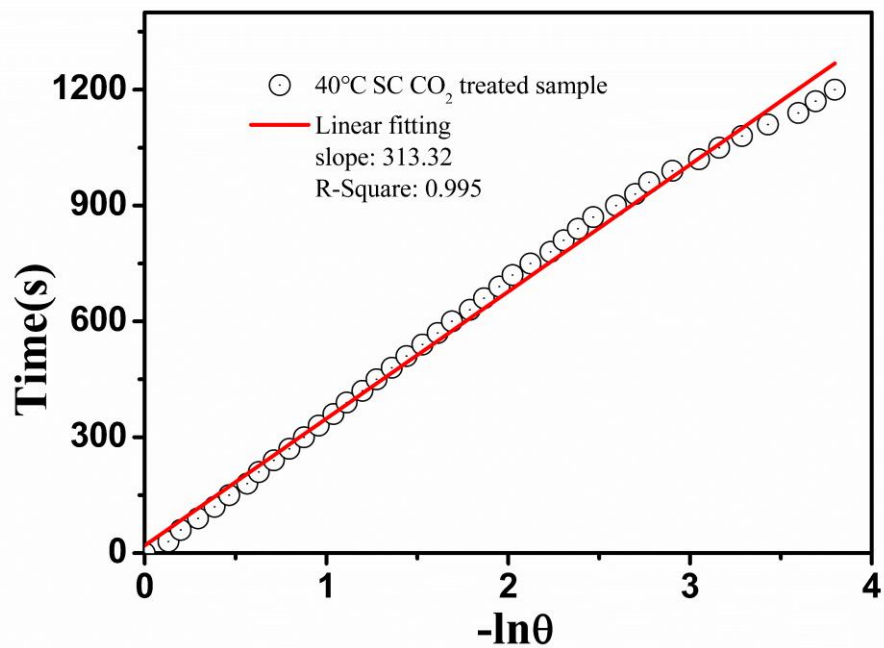


Figure S6. Plot of the cooling time versus the negative natural logarithm of the temperature driving force.

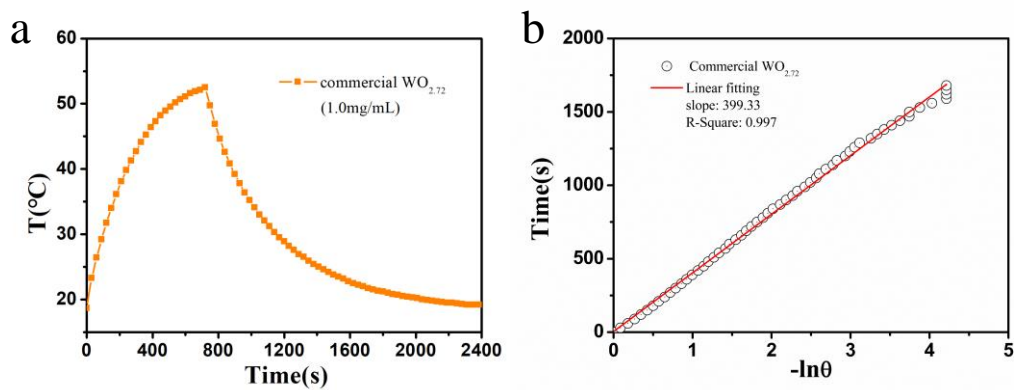


Figure S7. (a) Photothermal response of pristine  $\text{WO}_{2.72}$  sample under 808 NIR laser irradiation, and then the decay section was recorded after the laser was switched off. (b) Plot of the cooling time versus the negative natural logarithm of the temperature driving force.

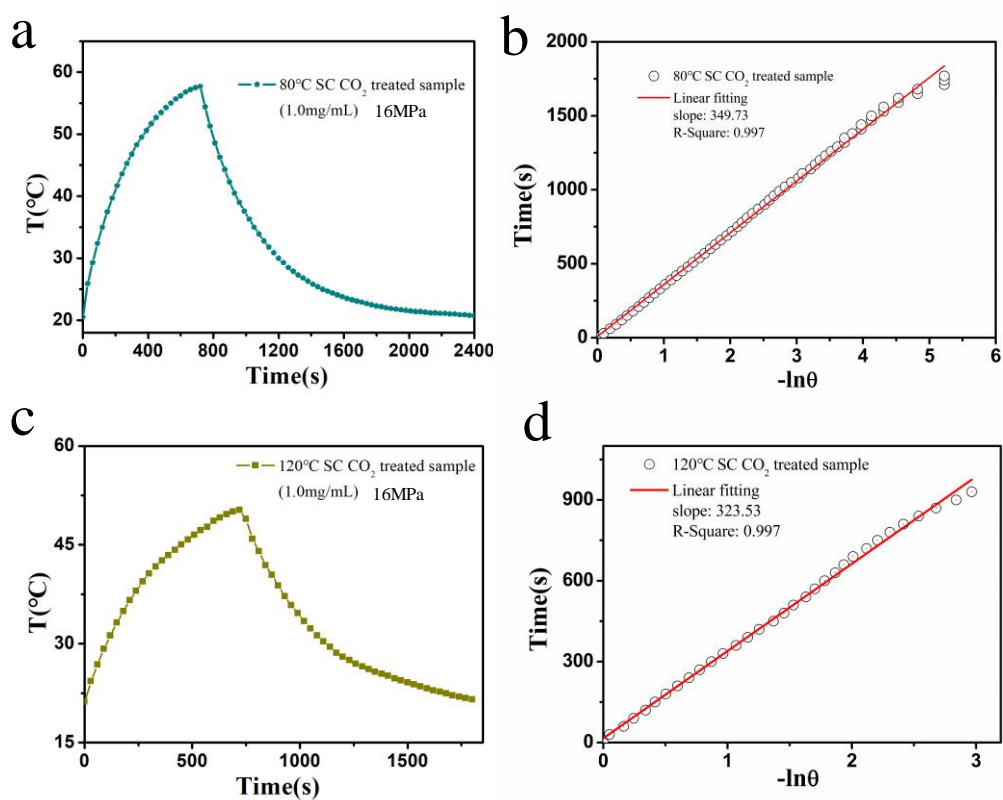


Figure S8. (a) (c) Photothermal response of SC CO<sub>2</sub> (80°C and 120°C) treated samples under 808 NIR laser irradiation, and then the decay section was recorded after the laser was switched off. (b) (d) Plot of the cooling time versus the negative natural logarithm of the temperature driving force.

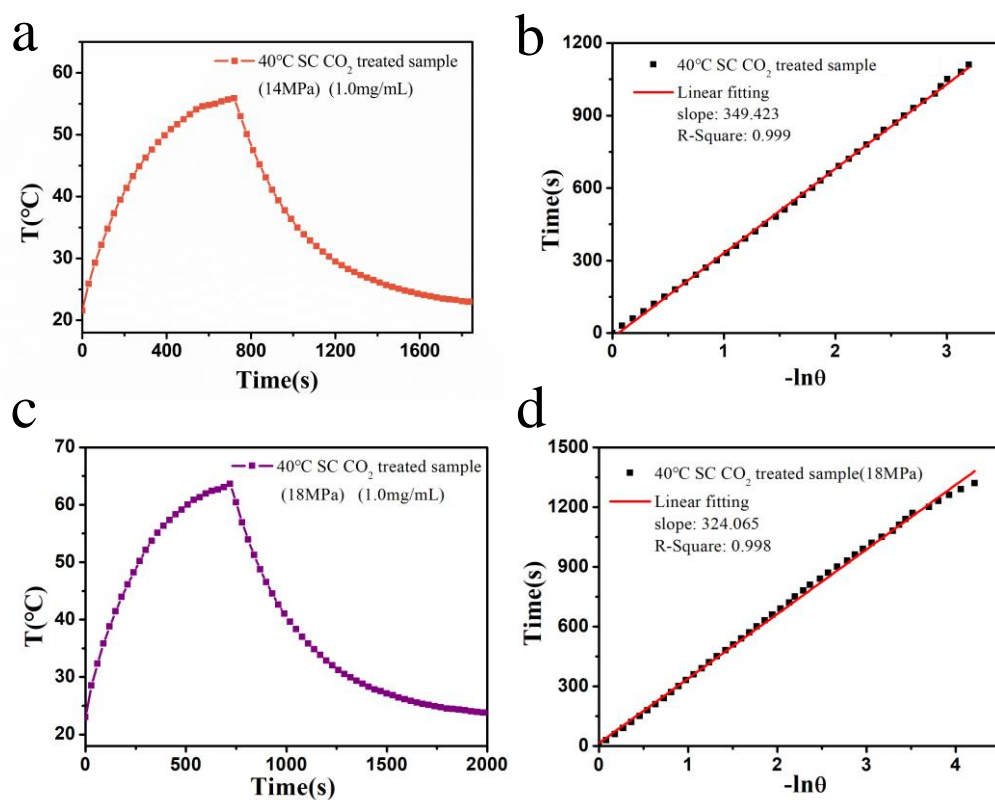


Figure S9. (a) (c) Photothermal response of SC CO<sub>2</sub> (14MPa and 18MPa) treated samples under 808 NIR laser irradiation, and then the decay section was recorded after the laser was switched off. (b) (d) Plot of the cooling time versus the negative natural logarithm of the temperature driving force.

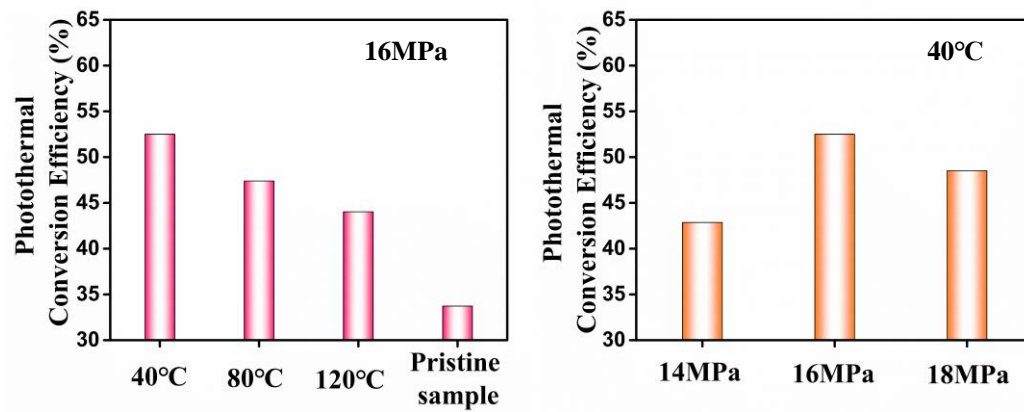


Figure S10. The photothermal conversion efficiency of pristine  $\text{WO}_{2.72}$  sample the SC  $\text{CO}_2$  treated sample at different temperature and pressure.

Table S1. The photothermal performance of different photothermal agents in recent years.

Photothermal catalyst	PCE	Laser wavelength	Literature source
Amorphous WO <sub>2.72</sub>	52.5%	808nm	This work
WO <sub>2.9</sub>	44.9%	808nm	Angew. Chem. Int. Ed. 2018, 57, 10666-10671.
Ultrasmall BPQDs	28.4%	808nm	Angew. Chem. Int. Ed., 2015, 54, 11526.
Dpa-melanin CNSs	40%	808nm	Adv. Mater., 2013, 25, 1353.
Ultrathin 2D Ti <sub>x</sub> Ta <sub>1-x</sub> S <sub>y</sub> O <sub>z</sub> nanosheets	39.2%	808nm	Angew. Chem. Int. Ed., 2017, 56, 7842-7846.
Ta <sub>2</sub> NiS <sub>5</sub> -P	35%	808nm	Small 2017, 13, 1604139.
Amorphous MoO <sub>3-x</sub>	61.8%	808nm	Chem. Commun., 2019, 55, 12527-12530.
Core-shell TiO <sub>2</sub>	55.2%	808nm	Nanoscale, 2017, 9, 16183.
Au NRs-Cu <sub>7</sub> S <sub>4</sub>	62%	808nm	Small, 2018, 14, 1703077